Reactions of Bis(pentafluorophenyl)borane with $Cp_2Ta(=CH_2)CH_3$: Generation and Trapping of Tantalocene Borataalkene Complexes

Kevin S. Cook,[†] Warren E. Piers,*[,†,1] Tom K. Woo,*[,‡] and Robert McDonald[§]

Department of Chemistry, University of Calgary, 2500 University Drive N.W., Calgary, Alberta, Canada T2N 1N4, Department of Chemistry, University of Western Ontario, London, Ontario, Canada N6A 5B7, and X-ray Structure Laboratory, Department of Chemistry, University of Alberta, Edmonton, Alberta, Canada T6G 2G2

Received May 9, 2001

Reaction of $Cp_2Ta(=CH_2)_3$ with 2 equiv of $HB(C_6F_5)_2$ results in production of the dihydride $Cp_2Ta(CH_2B(C_6F_5)_2)(\mu\text{-H})(H)$, **1**, plus 1 equiv of $H_3CB(C_6F_5)_2$. The pathway to **1** involves stepwise attack of borane first at the methylene group, followed by attack at the methyl group, which undergoes alkyl/hydride exchange with the second equivalent of $HB(C_6F_5)_2$. The product of $HB(C_6F_5)_2$ addition to the methylene ligand, methyl hydride complex $Cp_2Ta(CH_2B(C_6F_5)_2)(\mu\text{-H})(CH_3)$, **2**, can be intercepted by carrying out the reaction in hexane at low temperature, a medium in which it is nearly totally insoluble. This complex eliminates methane at higher temperatures in a first-order decomposition process ($\Delta H^{\ddagger} = 20.4(5)$ kcal mol^{-1} and $\Delta S^{\ddagger} = -2.0(2)$ cal mol^{-1} K^{-1}). The product, a borataalkene complex formulated as $Cp_2Ta[CH_2B(C_6F_5)_2]$, **3**, is unstable and cannot be isolated. DFT calculations support its formulation and show that it is present as a singlet/triplet mixture, accounting for the observed paramagnetism of solutions containing **3**. While **3** cannot be isolated or spectroscopically probed, it can be trapped if **2** is allowed to decompose in the presence of ^{t}BuNC or CO, giving the products $Cp_2Ta[\eta^2\text{-}CH_2B(C_6F_5)_2](L)$ (L = ^{t}BuNC, **4**; CO, **5**). Both of these compounds have been structurally characterized, and the structural and spectroscopic data for these compounds support an η^2 bonding description for the borataalkene ligand which is reminiscent of the commonly held Dewar−Chatt−Duncanson model for alkene bonding to transition metals. DFT calculations on **5** and the model complex $Cp_2Ta[\eta^2\text{-}CH_2BH_2](CO)$, **6**, provide further support for this description. The facile conversion of this ligand from an η^2 to an η^1 bonding mode is proposed to account for some H/D exchange processes observed in both dihydride **1** and methyl hydride complex **2**. Plausible mechanisms for both of these processes are proposed.

Introduction

The formal substitution of a carbon atom in an extended organic π system for a negatively charged boron has been a fruitful endeavor in both organoboron[2] and coordination chemistry. In the latter field, this transposition has allowed for the development of entire new families of ligands. For example, when this substitution is made in the benzene ring, the resulting "boratabenzene" [3] is now a negatively charged 6π electron system with better ligating properties toward transition metals than the neutral aromatic hydrocarbons. In addition, substitution at the boron center allows for considerable control over the electronic environment about the transition metal it is bonded to.[4] A similar modification to the $C_5H_5^-$ ligand leads to the borollides, a family of doubly negative Cp analogues with unique ligating properties.[5]

Beyond these two very prominent examples of turning hydrocarbyl ligands into "boratahydrocarbyl" ligands, less exploration has occurred. This applies particularly to the simplest of hydrocarbyl π ligands, olefins. Transposition of boron for carbon in ethylene gives borataethylene (eq 1), the simplest example of a wider class

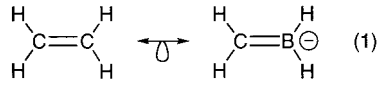

(1)

of compounds known as borataolefins. The borataalkene

[†] University of Calgary.
[‡] University of Western Ontario.
[§] University of Alberta.
(1) Phone: 403-220-5746. Fax: 403-289-9488. E-mail: wpiers@ucalgary.ca. S. Robert Blair Professor of Chemistry 2000−2005, E. W. R. Steacie Fellow 2001−2003.
(2) (a) Berndt, A. *Angew. Chem., Int. Ed. Engl.* **1993**, *32*, 985. (b) Eisch, J. J. *Adv. Organomet. Chem.* **1996**, *39*, 355.
(3) (a) Herberich, G. E.; Greiss, G.; Heil, H. F. *Angew. Chem., Int. Ed. Engl.* **1970**, *9*, 805. (b) Ashe, A. J., III; Shu, P. *J. Am. Chem. Soc.* **1971**, *93*, 1804. (c) Sullivan, S. A.; Sandford, H.; Beauchamp, J. L.; Ashe, A. J., III. *J. Am. Chem. Soc.* **1978**, *100*, 3737. (d) Herberich, G. E.; Ohst, H. *Adv. Organomet. Chem.* **1986**, *25*, 199. (e) Herberich, G. E.; Schmidt, B.; Englert, U. *Organometallics* **1995**, *14*, 471. (f) Qiao, S.; Hoic, D. A.; Fu, G. C. *J. Am. Chem. Soc.* **1996**, *118*, 6329.
(4) Bazan, G. C.; Cotter, W. D.; Komon, Z. J. A.; Lee, R. A.; Lachicotte, R. J. *J. Am. Chem. Soc.* **2000**, *122*, 1371.
(5) (a) Herberich, G. E. In *Comprehensive Organometallic Chemistry II*; Abel, E. W., Stone, F. G. A., Wilkinson, G., Eds.; Pergamon Press: Oxford, 1995; Vol. 1, p 197. (b) Sperry, C. K.; Cotter, W. D.; Lee, R. A.; Lachicotte, R. J.; Bazan, G. C. *J. Am. Chem. Soc.* **1998**, *120*, 7791.

10.1021/om010373o CCC: $20.00
Publication on Web 08/02/2001

Scheme 1

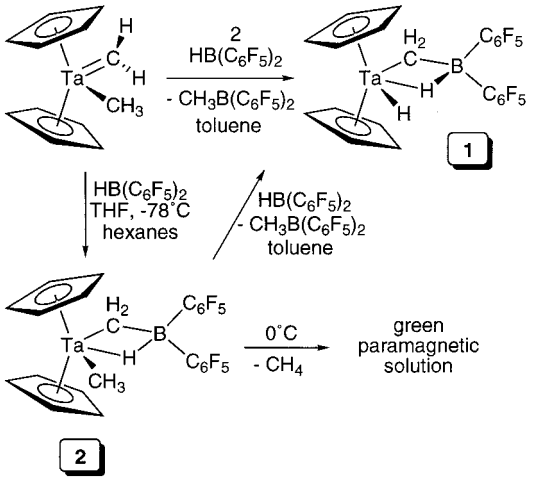

functionality has been implicated as being an important contributor to the products of the reduction of aryl boranes[6] and in the boron-Wittig reaction.[7] Furthermore, one example, $[Mes_2B{=}CH_2]^-[Li(12\text{-crown-}4)]^+$,[8] has been structurally characterized. Despite their viability, prior to our preliminary report[9] concerning the reactions of Sharp and Schrock's $Cp_2Ta(=CH_2)CH_3$[10] with the highly electrophilic borane $HB(C_6F_5)_2$,[11] there had been no reports of a well-defined borataalkene complex of a transtion metal.[12] Presumably, these anionic compounds should be capable of bonding to a metal in a fashion similar to the well-known Dewar−Chatt−Duncanson bonding mode of olefins.[13] In this full account we elaborate on the features of these reactions and delineate some of the chemistry of the borataalkene ligand $[H_2C{=}B(C_6F_5)_2]^-$.

Results and Discussion

Reactions of $Cp_2Ta(=CH_2)CH_3$ with $HB(C_6F_5)_2$. Like the reactions of dialkyl zirconocenes[14] with $HB(C_6F_5)_2$, the outcome of its reactions with Schrock's methylidene methyl tantalocene complex $Cp_2Ta(=CH_2)CH_3$ is strongly dependent on the reaction conditions employed, specifically solvent, temperature, and the equivalency of borane. Scheme 1 summarizes some of the chemistry involved. Treatment of $Cp_2Ta(=CH_2)CH_3$ with 2 equiv of borane in toluene or benzene at room temperature leads directly to the dihydride complex **1**, with concomitant formation of the methyl borane $H_3CB(C_6F_5)_2$, identified by its characteristic ^{1}H NMR signal at 1.32 ppm in benzene.[15] Complex **1** may be isolated free of this borane by recrystallization and washing with hexanes. Spectroscopically, complex **1** is characterized by large upfield shifts in the resonances for the carbon (6.9 ppm) and the protons (0.80 ppm) of the methylene unit in comparison to the starting material (10.14 and 224 ppm for the carbon and protons, respectively[10]). Also, two broadened signals for the terminal (0.15 ppm, whh = 12 Hz) and bridging (−3.27 ppm, whh = 51 Hz) hydrides are observed. We have previously reported the solid-state structure of **1**, which is clearly a dihydride complex in the ground state, since the H−H distance is 1.87 Å.[9]

Formation of **1** in this reaction occurs via two sequential reactions of $Cp_2Ta(=CH_2)CH_3$ with $HB(C_6F_5)_2$. This is demonstrated in part by the fact that, in other work, we have shown that the byproduct borane, $H_3CB(C_6F_5)_2$, reacts rapidly with $Cp_2Ta(=CH_2)CH_3$ via borane attack on the methylidene ligand, forming the zwitterionic complex $Cp_2Ta^+[CH_2B^-(CH_3)(C_6F_5)_2]CH_3$.[16] The absence of this product in the direct reaction of $Cp_2Ta(=CH_2)CH_3$ with 2 equiv of $HB(C_6F_5)_2$ suggests strongly that **1** is formed in a stepwise process involving electrophilic attack of the methylidene ligand by 1 equiv of borane, followed by an alkyl/hydride exchange between the tantalum methyl group and the second equivalent of borane. This is consistent with the fact that the HOMO in $Cp_2Ta(=CH_2)CH_3$ is largely associated with the methylidene ligand, while the HOMO-1 is concentrated on the methyl group. Schrock has demonstrated that other electrophiles (MeI, $AlMe_3$) attack the methylidene ligand preferentially;[10] attack by a second electrophile would necessarily take place at the methyl ligand.

The intermediate in this stepwise process can be intercepted under certain conditions in reactions involving $Cp_2Ta(=CH_2)CH_3$ and 1 equiv of borane. When these reagents are combined together (1:1 molar ratio) at room temperature in aromatic solvents, gas evolution is observed as the solution deepens in color to dark green. A clean product was not isolated from these reactions, and ^{1}H NMR spectroscopy was uninformative due to the paramagnetic nature of the species present in these solutions. In contrast, when this reaction is carried out in hexanes, an immediate tan precipitate is observed, which may be isolated via filtration and stored at −40 °C for several days without significant decomposition. Much spectroscopic and physical evidence suggests that this compound is the methyl hydride complex **2**. For example, solid-state ^{2}H NMR spectroscopy on d_1-**2**, generated in hexanes from $Cp_2Ta(=CH_2)CH_3$ and $DB(C_6F_5)_2$, gives a resonance at −0.28 ppm for the bridging deuteride (the chemical shift was confirmed by performing the experiment at two spin rates). Furthermore, tan solid **2** may be dissolved in d_8-THF at −50 °C without decomposition, and the ^{1}H and ^{13}C{^{1}H} NMR spectra obtained under these conditions are fully consistent with the structure shown. Specifically, upfield shifts are

(6) (a) Fiedler, J.; Zalis, S.; Klein, A.; Hornung, F. M.; Kaim, W. *Inorg. Chem.* **1996**, *35*, 3039. (b) Okada, K.; Teruhisa, K.; Masaji, O. *J. Chem. Soc., Chem. Commun.* **1995**, 233.

(7) Pelter, A.; Singaram, B.; Wilson, J. W. *Tetrahedron Lett.* **1983**, *24*, 643.

(8) Olmstead, M. M.; Power, P. P.; Weese, K. *J. Am. Chem. Soc.* **1987**, *109*, 2541.

(9) Cook, K. S.; Piers, W. E.; Rettig, S. J. *Organometallics* **1999**, *18*, 1575.

(10) Schrock, R. R.; Sharp, P. R. *J. Am. Chem. Soc.* **1978**, *100*, 2389.

(11) Parks, D. J.; Piers, W. E., Yap, G. P. A. *Organometallics* **1998**, *17*, 5492.

(12) Peripherally relevant compounds are the transition metal complexes of $R_2N{-}B{=}CR'_2$, in which the B=C bond is complexed to the metal center. Although $R_2N{-}B{=}CR'_2$ is a boraolefin, a resonance structure putting formal positive charge on N and negative charge on B gives this compound some borataolefin character. For a detailed discussion of the transition metal complexes of this particular ligand see: Helm, S. W.; Linti, G.; Nöth, H.; Channareddy, S.; Hofmann, P. *Chem. Ber.* **1992**, *125*, 73, and references therein.

(13) (a) Dewar, M. J. S. *Bull. Soc. Chem. Fr.* **1951**, *18*, C79. (b) Chatt, J.; Duncanson, L. A. *J. Chem. Soc.* **1953**, 2939.

(14) Spence R. E. v H.; Piers, W. E.; Sun, Y.; Parvez, M.; MacGillivray, L. R.; Zaworotko, M. J. *Organometallics* **1998**, *17*, 2459.

(15) Yang, X.; Stern, C. L.; Marks, T. J. *J. Am. Chem. Soc.* **1994**, *116*, 10015.

(16) (a) Cook, K. S.; Piers, W. E. Unpublished results. (b) Cook, K. S.; Piers, W. E.; Rettig, S. J.; McDonald, R. *Organometallics* **2000**, *19*, 2243.

Scheme 2

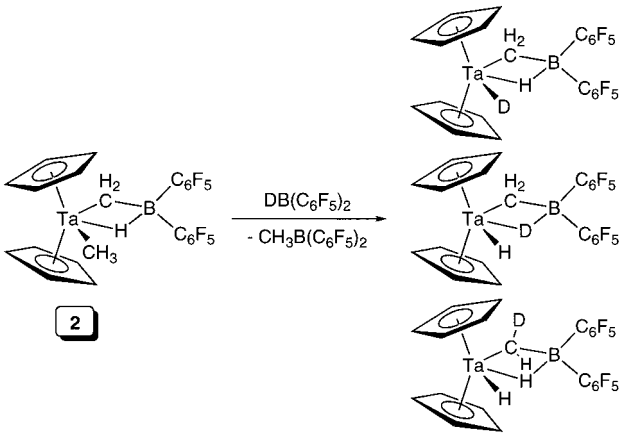

again observed for the methylidene protons (1.19 ppm) and carbon (20.5 ppm) nucleus. The bridging hydride appears at −1.54 ppm in the solution spectra, similar to the chemical shift observed for **1** in solution and d_1-**2** in the solid state. That the bridging hydride is located *cis* to the terminal methyl group is supported by a 2-D ROESY experiment, which shows cross-peaks between the bridging hydride and *both* the methyl and methylene groups, while indicating an absence of NOE between the outer hydrocarbyl groups. The physical evidence in support of **2** is the facility with which it undergoes reductive methane elimination; this process is described in detail below. The second step in the formation of dihydride **1** is effected by treatment of toluene solutions of **2** with another equivalent of $HB(C_6F_5)_2$, giving **1** and $H_3CB(C_6F_5)_2$. This step is quite facile in toluene or benzene in light of the aforementioned instability of **1** in solution at room temperature.

Attempts to prepare d_1-**1**, specifically labeled in the terminal hydride position, by treatment of methyl hydride **2** with $DB(C_6F_5)_2$ led to the observation of H/D exchange within **1** (Scheme 2). When d_1-**1** was worked up from this reaction (to fully remove $H_3CB(C_6F_5)_2$), ^2H NMR spectroscopy (Figure 1) showed that the deuterium is found not only in the terminal hydride position, but also in the bridging position *and* the methylene site. Figure 1a shows that, at short reaction time, the majority of the label is found in the terminal hydride position, but over time, the deuterium washes into the other positions until, after about 60 h, the distribution is as shown in Figure 1c. The final distribution of 3.5:1.3:1.0 (Ta−C(H)D:Ta−D_t:Ta−D_b) is skewed from the statistical 2:1:1 ratio due to an equilibrium isotope effect favoring deuterium in the methylene position. Since no deuterium is incorporated into the $H_3CB(C_6F_5)_2$ byproduct, the scrambling likely occurs within **1** after its formation; a proposed mechanism for this process is discussed below.

As mentioned above, in the absence of another equivalent of $HB(C_6F_5)_2$, methyl hydride compound **2** undergoes facile, exothermic reductive elimination of methane from **2** commencing at temperatures around −20 °C; interestingly, elimination of $H_3CB(C_6F_5)_2$ is not a competing process under these conditions. The reductive elimination can be followed quantitatively by ^1H NMR spectroscopy using Cp_2Fe as an internal standard to monitor the loss of [**2**] over time. Although the product(s) is (are) paramagnetic, the signals for diamagnetic **2** remain sharp throughout the reaction.[17] The rate was evaluated over the temperature range −10 to +20 °C. Representative first-order plots at various temperatures within this range are given in Figure 2a, while an Eyring plot is shown in Figure 2b; the activation parameters are $\Delta H^{\ddagger} = 20.4(5)$ kcal mol^{-1} and $\Delta S^{\ddagger} = -2.0(2)$ cal mol^{-1} K^{-1}. The former is at the low end of the range of values that has been reported for methane eliminations,[18] while the latter is somewhat more negative than normal. Typically $\Delta S^{\ddagger}$ values are 5−10 eu in reductive eliminations due to the dissociative nature of the reaction. In this system, the transition state may be more ordered because of the Lewis acidic borane center; however, since we were only able to follow this reaction over a relatively narrow temperature range, caution must be exercised in the interpretation of $\Delta S^{\ddagger}$. The observed rate constant for loss of CD_4 from d_6-**2** (formed from $Cp_2Ta(=CD_2)CD_3$ and $DB(C_6F_5)_2$) gave a k_H/k_D kinetic isotope effect of 1.57(4) at 10 °C,[19] a value in line with the range of 1.5−3.0 found for various *exothermic* reductive eliminations.[20]

Attempts to measure the primary kinetic isotope effect for this reaction by allowing d_1-**2** (with deuterium in the bridging hydride position) to undergo methane

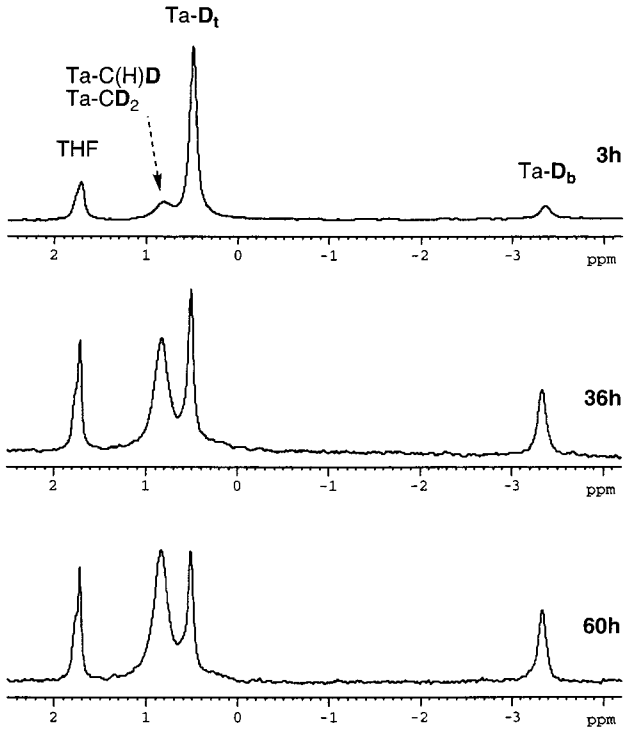

Figure 1. $^2H\{^1H\}$ NMR spectra of d_1-**1** over time. (a) First spectrum after workup of d_1-**1** ($t \approx 3$ h). (b) $t = 36$ h. (c) $t = 60$ h.

(17) Methane loss from **2** was also followed under pseudo-first-order conditions using an excess of ^{t}BuNC as a trapping agent (vide infra). The rate constants obtained were the same within experimental error, so methane loss at various temperatures was monitored without the trapping agent.

(18) (a) *cis*-$Pt(H)(CH_3)(PPh_3)_2$ $\Delta G^{\ddagger} = 18.2$ kcal mol^{-1}: Halpern, J. *Acc. Chem. Res.* **1982**, *15*, 332. (b) $(C_5Me_5)_2W(CH_3)(H)$ $\Delta H^{\ddagger} = 29.3(8)$ kcal mol^{-1}, $\Delta S^{\ddagger} = 1.5(20)$ eu: Parkin, G.; Bercaw, J. E. *Organometallics* **1989**, *8*, 1172. (c) $[Pd_2Me_2(\mu\text{-}H)(\mu\text{-}dppm)_2]PF_6$ $\Delta H^{\ddagger} = 29.9(10)$ kcal mol^{-1}, $\Delta S^{\ddagger} = 10(5)$ eu: Stockland, R. A.; Anderson, G. K.; Rath, N. P. *J. Am. Chem. Soc.* **1999**, *121*, 7945. (d) $Os(CO)_4(H)CH_3$ $\Delta H^{\ddagger} = 21.9(5)$ kcal mol^{-1}, $\Delta S^{\ddagger} = -8(1)$ eu: Okrasinski, S. J.; Norton, J. R. *J. Am. Chem. Soc.* **1977**, *99*, 295. (e) $Cp_2W(H)CH_3$ $\Delta H^{\ddagger} = 25.1(3)$ kcal mol^{-1}, $\Delta S^{\ddagger} = -4(1)$ eu: Bullock, R. M.; Headford, C. E.; Hennessy, K. M.; Kegley, S. E.; Norton, J. R. *J. Am. Chem. Soc.* **1989**, *111*, 3897.

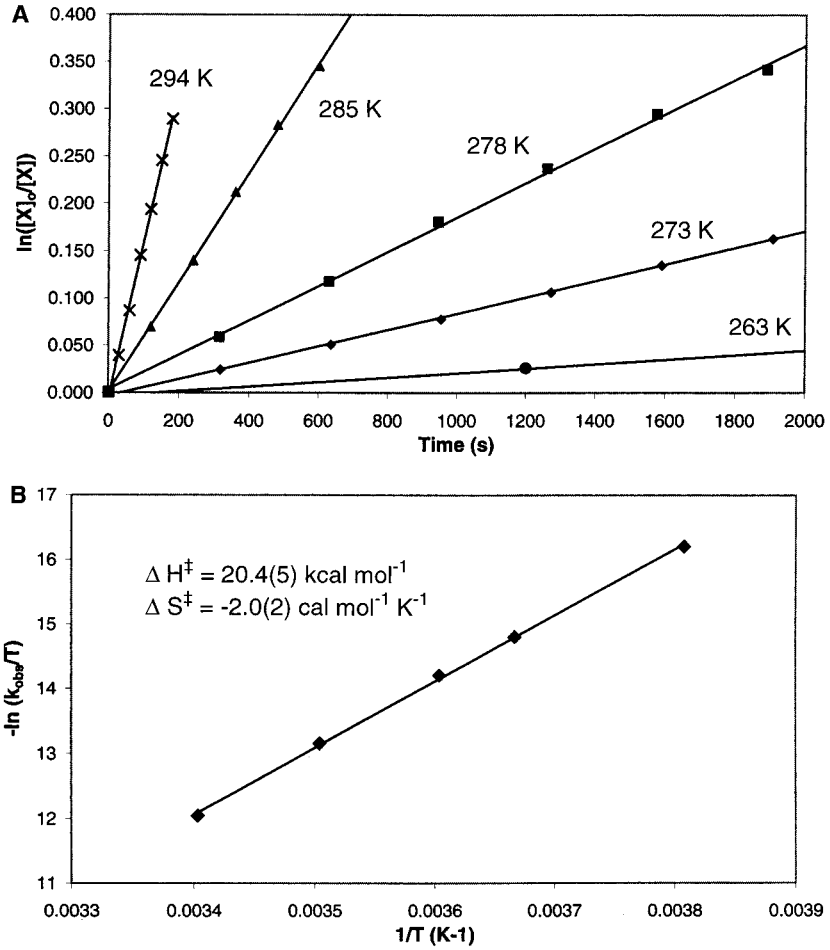

Figure 2. (a) Representative first-order kinetic plots of the loss of methane from **2**. Each of these reactions was followed to at least 5 half-lives, although the full data set is not shown for each run. (b) Eyring plot of the rate constants obtained.

loss gave an artificially low k_H/k_D of 1.15(4), due to an exchange process related to that discovered for dihydride **1**. Specifically, at temperatures where CH_3D loss was not occurring (−78 °C), the bridging deuteride label was observed to wash into the methyl group of **2**, where it is both statistically and thermodynamically favored. Even at these temperatures, this process is relatively facile. Notably, no deuterium is scrambled into the methylene position of **2** under these conditions. Since exchange of deuterium into the methylene group occurred only slowly at room temperature in **1**, we conclude that transfer of deuterium to the methyl position is kinetically favored over scrambling into the methylene moiety. The mechanism of this exchange process is described in more detail below.

The Nature of Borataalkene Complex 3: Trapping Experiments. Although we have not been able to characterize the green paramagnetic material that arises from CH_4 loss from **2**, trapping experiments and computational studies strongly suggest that it is the "borataalkene" complex **3** (Scheme 3). As shown in the scheme, when **2** is allowed to undergo elimination of methane in the presence of excess *tert*-butyl isocyanide, or 1 atm of carbon monoxide, the products **4** and **5** can be isolated in excellent yield. Clean reactions are not observed when the trapping agent is a strong σ donor, such as PMe_3 or pyridine; only π acceptor ligands effectively fulfill a trapping role in this chemistry. It is also important to note that no trace of the products $Cp_2Ta(L)CH_3$, both of which are related to known compounds (L = ^{t}BuNC;[21] L = CO[22]) or $H_3CB(C_6F_5)_2$·CNR,[23] is observed in these reactions, again indicating selective loss of CH_4 from **2**.

Both of the trapped products **4** and **5** have been characterized crystallographically; complex **4** was reported earlier and an ORTEP diagram of CO trapped product **5** is given in Figure 3. Table 1 contains metrical data for both complexes for comparison. In each species, the borataalkene ligand is bound in an unsymmetrical η^2-bonding mode. In two related titanium complexes, **I**[24] and **II**[25] (Chart 1), which have both been crystallographically characterized,[26] the borataalkene ligand

(19) The value of 1.57 obtained in this experiment is a combination of the primary and secondary effects associated with deuterium labels in the CD_2 and particularly the CD_3 positions; these secondary effects are expected to be small.

(20) Halpern, J. *Acc. Chem. Res.* **1982**, *15*, 332.

(21) Klazinga, A. H.; Teuben, J. H. *J. Organomet. Chem.* **1980**, *192*, 75.

(22) (a) Klazinga, A. H.; Teuben, J. H. *J. Organomet. Chem.* **1979**, *165*, 31. (b) Klazinga, A. H.; Teuben, J. H. *J. Organomet. Chem.* **1980**, *194*, 309.

(23) Jacobsen, H.; Berke, H.; Döring, S.; Kehr, G.; Erker, G.; Fröhlich, R.; Meyer, O. *Organometallics* **1999**, *18*, 1724.

(24) Scollard, J. D.; McConville, D. H.; Rettig, S. J. *Organometallics* **1997**, *16*, 1810.

(25) Zhang, S.; Piers, W. E.; Gao, X.; Parvez, M. *J. Am. Chem. Soc.* **2000**, *122*, 5499.

(26) For another example of a titanium compound with this ligand bound in an η^1 mode see: Thorn, M. G.; Vilardo, J. S.; Fanwick, P. E.; Rothwell, I. P. *Chem. Commun.* **1998**, 2427.

Scheme 3

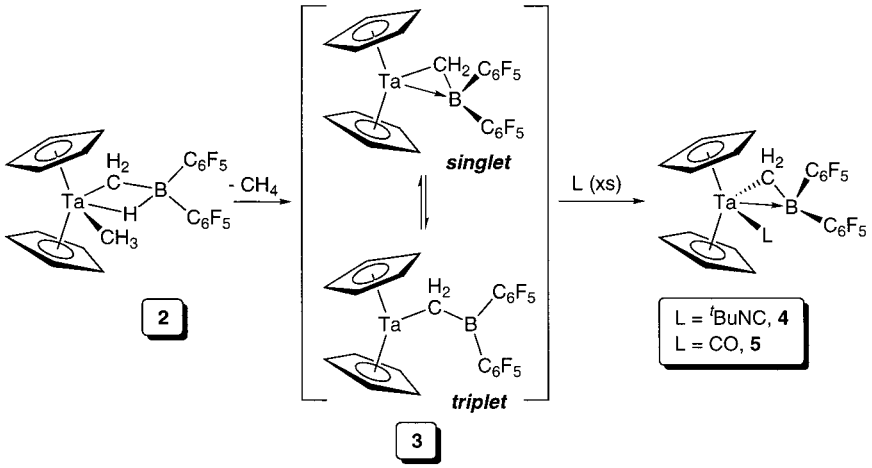

Table 1. Selected Metrical Parameters for 4 and 5

4		5	
	Bond Distances (Å)		
Ta(1)−Cp(1)[a]	2.086	Ta−Cp(1)[b]	2.065
Ta(1)−Cp(2)[c]	2.084	Ta−Cp(2)[d]	2.062
Ta(1)−B(1)	2.738(6)	Ta−B	2.728(6)
Ta(1)−C(16)	2.348(5)	Ta−C(2)	2.337(5)
Ta(1)−C(11)	2.075(5)	Ta−C(1)	2.058(6)
C(11)−N(1)	1.164(6)	C(1)−O	1.158(6)
C(12)−N(1)	1.486(6)		
C(16)−B(1)	1.525(7)	C(2)−B	1.508(8)
C(17)−B(1)	1.595(8)	C(21)−B	1.603(7)
C(23)−B(1)	1.623(7)	C(31)−B	1.605(7)
	Bond Angles (deg)		
Cp(1)−Ta(1)−Cp(2)[a,c]	133.3	Cp(1)−Ta−Cp(2)[b,d]	134.6
C(11)−Ta(1)−C(16)	100.4(2)	C(1)−Ta−C(2)	104.84(19)
C(11)−Ta(1)−B(1)	66.8(2)	C(1)−Ta−B	71.6(2)
C(16)−Ta(1)−B(1)	33.8(2)	C(2)−Ta−B	33.4(2)
Ta(1)−C(16)−B(1)	87.3(3)	Ta−C(2)−B	87.6(3)
Ta(1)−C(11)−N(1)	171.2(4)	Ta−C(1)−O	169.9(5)
C(11)−N(1)−C(12)	136.0(5)		
Ta(1)−B(1)−C(16)	58.9(3)	Ta−B−C(2)	58.8(3)
Ta(1)−B(1)−C(17)	113.2(3)	Ta−B−C(21)	114.2(3)
Ta(1)−B(1)−C(23)	119.7(4)	Ta−B−C(31)	119.0(3)
C(16)−B(1)−C(17)	124.7(5)	C(2)−B−C(21)	123.5(4)
C(16)−B(1)−C(23)	115.7(5)	C(2)−B−C(31)	117.3(4)
C(17)−B(1)−C(23)	113.7(4)	C(21)−B−C(31)	113.2(5)

[a] Cp(1) is the centroid for C(1)−C(5). [b] Cp(1) is the centroid for C(10)−C(14). [c] Cp(2) is the centroid for C(6)−C(10). [d] Cp(2) is the centroid for C(15)−C(19).

functions only as a σ donor. The alkene-like bonding of $[CH_2B(C_6F_5)_2]^-$ in **4** and **5** is supported by at least five observations. (1) The Ta−CH_2 distances are slightly longer than a typical Ta−C σ bond (cf. the Ta−CH_3 distance of 2.268(1) Å in $Cp_2Ta(=CH_2)CH_3$[27] or the Ta−CH_2R distance of 2.29(1) Å in $Cp_2Ta(\eta^2\text{-}C_8H_8)CH_2CH_2\text{-}CH_3$[28]), as would be expected upon approaching an η^2 bonding mode (the Ta−C distances to the η^2-C_8H_8 ligand in the latter complex above are 2.33(2) and 2.32(1) Å). (2) The acute Ta−CH_2−B bond angles (87.3(3)° and 87.6(3)° for **4** and **5**, respectively) suggest a Ta−B interaction and are markedly different from the analogous angles in **I** (125.1(3)°) and **II** (110.8(3)°), which are more consonant with sp^3 hybridization at carbon. (3) The Ta−B distances of 2.738(6) and 2.728(6) Å for **4** and **5**, while quite long in comparison to those found for

Chart 1

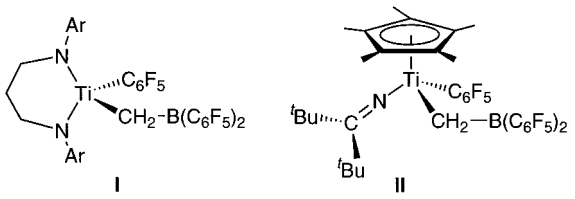

Ta−B σ bonds (≈2.26−2.29 Å[29]), are suggestive of an attractive Ta−B interaction. This is further implied by the slight pyramidalization of the boron center ($\sum_{C-B-C}$ = 354.1° for **4** and **5**); in **I** and **II**, this sum is 360° and the boron centers are planar. (4) The B−C bond distances of 1.525(7) and 1.508(8) Å are intermediate between typical $B-C_{sp3}$ bond distances (1.578 Å for BMe_3[30]) and that of 1.444 Å found in $[Mes_2B{=}CH_2]^-[Li\text{-}12\text{-crown-}4]^+$, as would be expected in a Dewar−Chatt−Duncanson type η^2 bonding situation. (5) Finally, the C=X stretching frequencies for the trapping ligand (X = N^{t}Bu, 1882 cm^{-1}, **4**; O, 1923 cm^{-1}, **5**) are both higher than would be expected for $Cp_2Ta(L)R$ derivatives, where R is a conventional hydrocarbyl σ donor. This indicates that the π electrons on tantalum are being shared between the CX ligand and the borataalkene ligand, which must be acting as a π acceptor in some capacity.

The η^2 bonding mode for this ligand is also maintained in solution, as evidenced by the ^{11}B and ^{19}F NMR spectra. The chemical shift of the ^{11}B nucleus is roughly indicative of the coordination environment about boron.[31] While the values found for compounds **I** and **II** (79.4 and 51.8 ppm, respectively) are consistent with neutral, three-coordinate boron, the shifts observed for **4** and **5** are 8.5 and 7.2 ppm. These values are more consistent with neutral, higher coordinate boron centers, reflecting the presence of a Ta−B interaction. Furthermore, in $B-C_6F_5$ compounds, the chemical shift difference between the *meta* and *para* fluorine atoms in the ^{19}F NMR spectrum has also been used to infer the boron center's ability to delocalize π electron density from the *para* fluorine atoms.[32] The values of $\Delta\delta_{m,p}$ for **I** and **II**

(27) Takusagawa, F.; Koetzle, T. F.; Sharp, P. R.; Schrock, R. R. *Acta Crystallogr. Ser. C* **1988**, *44*, 439.
(28) Van Bolhuis, F.; Klazinga, A. H.; Teuben, J. H. *J. Organomet. Chem.* **1981**, *206*, 185.
(29) Lantero, D. R.; Motry, D. H.; Ward, D. L.; Smith, M. R., III. *J. Am. Chem. Soc.* **1994**, *116*, 10811.
(30) Bartell, L. S.; Carroll, B. L. *J. Chem. Phys.* **1965**, *42*, 3076.
(31) Kidd, R. G. In *NMR of Newly Accessible Nuclei*; Laszlo, P. Ed.; Academic Press: New York, 1983; Vol. 2.

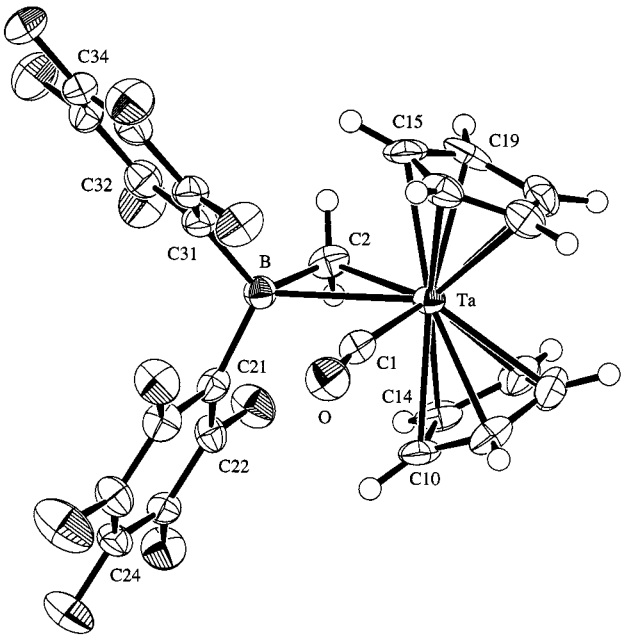

Figure 3. ORTEP diagram of **5** (50% ellipsoids).

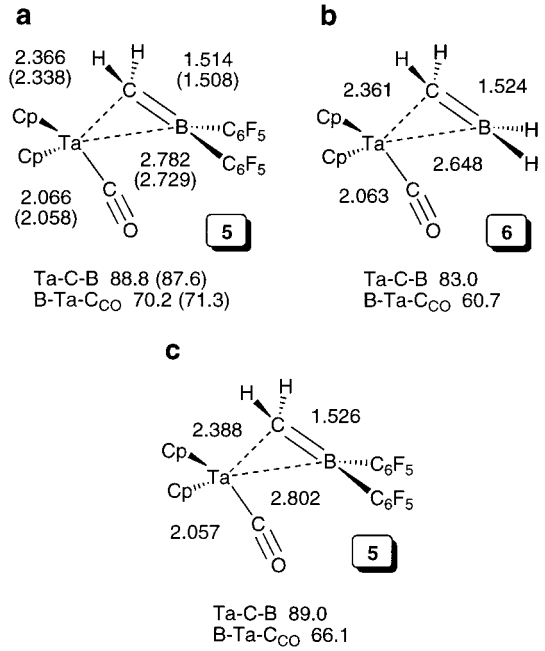

Figure 4. Summary of geometric parameters of the calculated structures of (a) complex **5**, $Cp_2Ta(\eta^2\text{-}CH_2B(C_6F_5)_2)CO$, and (b) the model complex **6**, $Cp_2Ta(\eta^2\text{-}CH_2BH_2)CO$. (c) Combined QM/MM structure of **5**. The parenthetic values displayed in (a) are the values measured in the X-ray structure. Bond distances reported in angstroms.

are 10.2 and 7.5 ppm;[33] in **4** and **5**, they are smaller (5.1 and 5.4 ppm), indicating that the boron center in these compounds is less able to accept electron density from the $-C_6F_5$ rings, due to its interaction with the tantalum centers.

Finally, the borataalkene bonding was also examined within the framework of molecular orbital theory through Kohn−Sham DFT calculations. In particular, we have examined the bonding in **5** and a model of it, $Cp_2Ta(\eta^2\text{-}CH_2BH_2)CO$, **6**, where the pentafluorophenyl substituents on the boron center are replaced with hydrogens. Important geometric parameters of the optimized DFT structure of **5** and the model complex **6** are shown in Figures 4a and 4b, respectively. The model complex exhibits a tighter borataalkene complexation to the Ta center, as shown by the slightly shorter Ta−B distance and the smaller Ta−C−B angle. Also shown in Figure 4a are the geometric parameters from the X-ray structure, which show excellent agreement with the DFT structure.

A molecular orbital analysis of **5** and **6** is consistent with a η^2 bonding mode for the borataalkene. Shown in Figure 5a is the Kohn−Sham molecular orbital of the model complex that is indicative of the η^2-borataalkene to Ta bonding (the orbitals in **5** are comparable). Shown in Figure 5b is the highest occupied molecular orbital that can be characterized as primarily a Ta-carbonyl "back-bonding" orbital. Figure 5b suggests there is also a small, but not insignificant interaction with a linear combination of the π and π^* orbitals of the borataalkene.[34] This π-acceptor interaction of the borataalkene is consistent with the aforementioned C═O stretching frequencies.

As previously mentioned, the B−Ta distance in **6** is shortened compared to pentafluorophenyl-substituted complex **5**. One question that arises is whether this effect is an electronic or steric effect of the pentafluorophenyl substituents. To investigate this question, we have performed a combined quantum mechanics and molecular mechanics (QM/MM) calculation[35] where the pentafluorophenyl groups were treated in the molecular

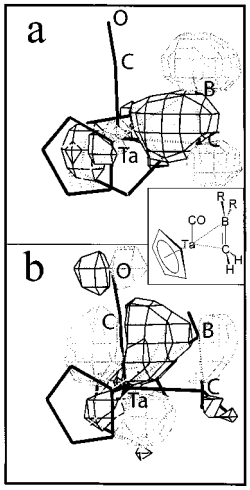

Figure 5. Isosurface plots of the Kohn−Sham molecular orbitals of $Cp_2Ta(\eta^2\text{-}CH_2BH_2)CO$. The molecular orbital shown in (a) is characterized as a Ta-borataalkene bonding orbital. The highest occupied molecular orbital is shown in (b). The inset depicts the orientation of the molecule in both isosurface plots. Hydrogens on the Cp rings have been omitted for clarity, and an isosurface value of 0.04 au was used.

(32) Horton, A. D.; de With, J. *Organometallics* **1997**, *16*, 5424.

(33) This value is an average of two since the $-C_6F_5$ rings in **II** are diastereotopic.

(34) The makeup of the HOMO has been examined in more detail by a calculation of $Cp_2Ta(CH_2BH_2)CO$, in which the molecular orbitals of the $H_2C{=}BH_2^-$ and the Cp_2TaCO^+ fragments were used as a basis set. By using this procedure, we can in the framework of molecular orbital theory quantify the contribution of the borataalkene π and π^* orbitals to the HOMO. The molecular orbital eigenvector coefficients for the π and π^* orbitals of the borataalkene were determined to be 0.13 and 0.18, respectively.

mechanics region. In this model, only the steric influence of the pentafluorophenyl substituents are accounted for. Use of the combined QM/MM method as a tool to separate steric from electronic effects has been previously demonstrated.[36] Figure 4c summarizes the important geometric parameters from the QM/MM calculation of complex **5**. The Ta−B distance from the QM/MM simulation is 2.8 Å, which is slightly longer than the Ta−B distance of 2.78 Å measured in the full DFT structure. This suggests that the elongated Ta−B distance in the pentafluorophenyl complex is primarily due to steric pressure from the bulky aryl substituents. The steric elongation of the Ta−B bond distance is therefore further evidence of a preference for a η^2 bonding mode in **5**.

While the above discussion is fairly convincing in its cumulative effect, it must be said that the evidence also suggests that the η^2 bonding of this borataalkene ligand is fairly tenuous. In addition to the steric issues discussed above, the greater electronegativity of C vs B dictates that the occupied molecular orbitals of the borataalkene are emphasized at carbon, creating an electronic impetus for σ bonding through an ylide-like resonance structure, i.e., $[CH_2-B(C_6F_5)_2]^-$, where the negative charge is more localized on carbon. Thus, when there are no d electrons present (as in **I** and **II**, for example), η^1 bonding is the natural mode for this ligand type.

Nature of Borataalkene Complex 3: DFT Calculations. The putative complex **3** is isoelectronic to the known, diamagnetic, ethylene derivative $Cp^*_2Ti(\eta^2\text{-}C_2H_4)$,[37] and so it is unclear why this compound would be paramagnetic. Since we were unable to isolate any clean product corresponding to **3**, we turned to DFT calculations in order to probe its nature in more detail. These experiments suggest that the observed paramagnetism of solutions containing **3** may be due to this ligand's dual bonding tendencies, as exemplified by compounds **4**/**5** vs **I**/**II**, i.e., as a π-acidic olefin-type donor or a σ-bonding alkyl-type donor. While an η^2-bound species $Cp_2Ta[\eta^2\text{-}CH_2B(C_6F_5)_2]$ might be expected to be diamagnetic (by analogy to $Cp^*_2Ti(\eta^2\text{-}C_2H_4)$), it is entirely likely that $Cp_2Ta[\eta^1\text{-}CH_2B(C_6F_5)_2]$ would be a high-spin, paramagnetic species. To our knowledge, monomeric compounds of general formula "Cp_2TaR" have not been isolated, but related niobium derivatives have been reported as adopting high-spin ground states.[38]

Accordingly, DFT calculations were performed on singlet and triplet states for $Cp_2Ta[CH_2B(C_6F_5)_2]$, and their structural features evaluated. The energies of these two states were found to be very close, differing only by about 1.5 kcal mol^{-1}, and in fact the triplet was found to be the lower energy species. However, the energetic proximity of the two species suggests that an equilibrium mixture of the two under ambient conditions is likely. Figure 6 shows the structures (a, singlet; b triplet) along with selected metrical data; a full listing of the Cartesian coordinates for these structures is given in the Supporting Information. In the singlet, the borataalkene ligand adopts an η^2 bonding mode with structural features similar to those observed in compounds **4** and **5**. Specifically, the Ta−C−B angle of 86° is very close to those observed in the Lewis base adducts of **3**, as is the Ta−B distance of 2.75 Å. As in **4** and **5**, the boron center is slightly pyramidalized due to its interaction with the Ta center. The ligand is slightly offset from the bisecting vector of the bent tantalocene moiety to accommodate a weak Ta−F interaction with one of the *ortho* fluorine atoms of a boron $-C_6F_5$ ring; the calculated distance is 2.38 Å. Effectively, this fluorine interaction functions as the trapping ligand L in **4** and **5**, blocking the third metallocene orbital/coordination site.

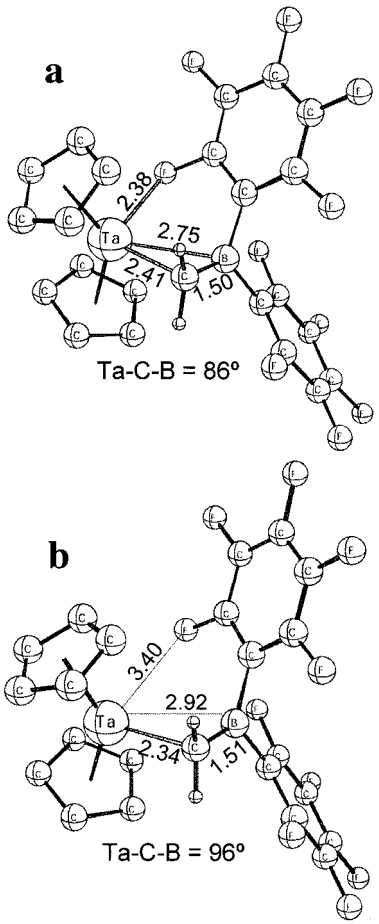

Figure 6. Unrestricted DFT(Becke-Perdew86) geometries of $Cp_2Ta[CH_2B(C_6F_5)_2]$, **3**. (a) singlet; (b) triplet. Bond distances reported in angstroms. Hydrogen atoms on the Cp rings have been omitted for clarity.

In contrast, the slightly more stable triplet assumes a bonding mode more consistent with η^1 attachment of the borataalkene ligand. This is indicated by a more open Ta−C−B angle of 96° and an elongated Ta−B distance of 2.92 Å. Furthermore, the Ta−C distance of 2.34 Å is more in line with normal Ta−C_{sp3} bond lengths and is slightly shorter than the distance calculated for the singlet and found for **4**/**5**. The boron center in the triplet is effectively planar, and there are no significant Ta−F interactions (the shortest Ta−F contact is 3.40 Å) owing to the single occupancy of the two orbitals available for coordination of further ligands. These results account for the paramagnetic nature of the

(35) Maseras, F. *Chem. Commun.* **2000**, 1821.
(36) Woo, T. K.; Pioda, G.; Rothlisberger, U.; Togni, A. *Organometallics* **2000**, *19*, 2144.
(37) Cohen, S. A.; Auburn, P. R.; Bercaw, J. E. *J. Am. Chem. Soc.* **1983**, *105*, 1136.
(38) Otto, E. E. H.; Brintzinger, H. H. *J. Organomet. Chem.* **1979**, *170*, 209.

Scheme 4

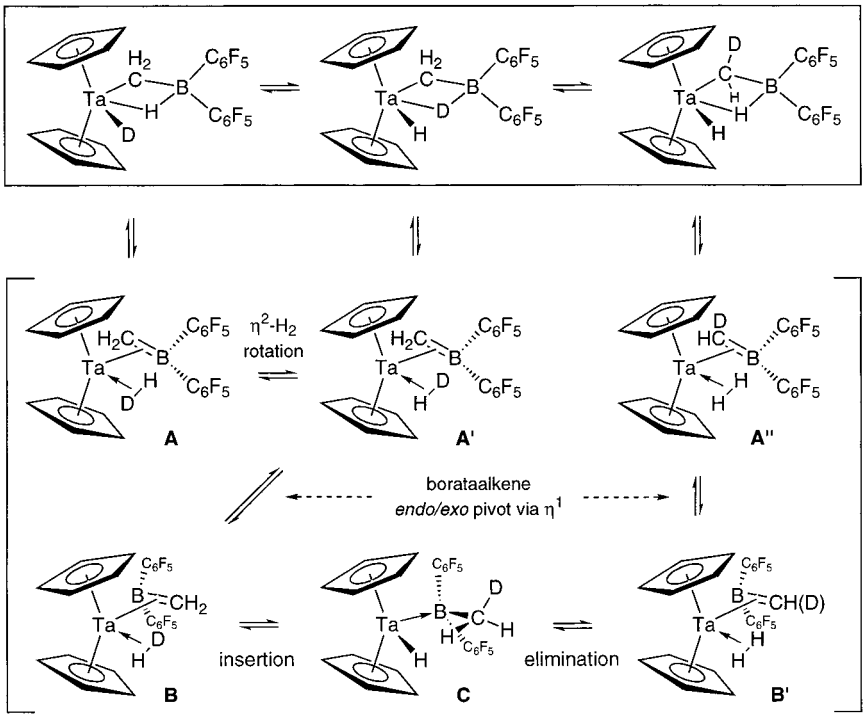

solutions which we believe to contain **3**; however, it is likely that the triplet is kinetically prone to decomposition, which is why we have been unable to isolate any material from these solutions.

Boratalkene-Mediated Mechanisms of H/D Exchange in 1 and 2. The accessibility of weakly π-accepting η^2-boratalkene and strongly σ-donating η^1-boratalkene structures suggests that they may be involved in the mechanisms for the deuterium scrambling processes observed in **1** and **2**. In **1**, two processes must be operative; Scheme 4 shows the proposed mechanisms. While **1** is clearly a conventional dihydride complex in the ground state, exchange between the terminal and bridging hydrides probably occurs through a short-lived Ta(III) η^2-dihydrogen complex (**A**) via rotation of the dihydrogen ligand. Although d^2 dihydrogen complexes are rare,[39] some examples have been reported. The most studied examples are in fact niobocene[40] and tantalocene[41] derivatives related to the intermediate **A** proposed in Scheme 4. In these systems, rotation of the η^2-H_2 ligand has been shown to have a moderately high barrier ($\approx$9−11 kcal mol^{-1}), but exchange does occur under ambient conditions. It should be noted that, for most of the tantalocene derivatives reported, dihydride structures are strongly favored, but η^2-dihydrogen intermediates are implicated by chemical exchange processes and quantum exchange couplings observed in the ^{1}H NMR spectra.[42] The one definitive d^2-tantalocene dihydrogen complex, Chaudret's cationic $[Cp_2Ta(\eta^2\text{-}H_2)CO]^+[BF_4]^-$, is stabilized by the electron-deficient nature of the metal center and the π-acidic properties of the CO ligand. Possibly, the weakly π-acidic η^2-$CH_2B(C_6F_5)_2$ ligand performs a stabilizing role for this dihydrogen intermediate.

Exchange of deuterium into the methylene position of **1** most reasonably occurs from the bridging position, and we again propose that it begins with slippage of the ground-state structure of **1** into an η^2-boratalkene intermediate (i.e., **A′**) as shown in Scheme 4. This species may pivot through an η^1 structure to the isomer in which the $B(C_6F_5)_2$ end of the molecule occupies an *exo* position of the metallocene wedge (**B**). Deuterium may scramble into the methylene position via an insertion/elimination sequence as shown, giving **B′** and **A″**, where deuterium is now in the methylene position. This mechanism would require that the $H_3CB(C_6F_5)_2$ moiety formed upon insertion remains associated with the tantalum center, presumably via donation of the tantalum d^2 electrons to the boron center, i.e., **C**.[43]

The lower energy exchange of deuterium from the bridging deuteride position into the methyl group of **2**

(39) (a) Jessop, P. G.; Morris, R. H. *Coord. Chem. Rev.* **1992**, *121*, 155. (b) Sabo-Etienne, S.; Chaudret, B. *Chem. Rev.* **1998**, *98*, 2077.

(40) (a) Heinekey, D. M. *J. Am. Chem. Soc.* **1991**, *113*, 6074. (b) Antinolo, A.; Carrillo-Hermosilla, F.; Chaudret, B.; Fajardo, M.; Fernandez-Baeza, J.; Lanfranchi, M.; Limbach, H.-H.; Maurer, M.; Otero, A.; Pellinghelli, M. A. *Inorg. Chem.* **1996**, *35*, 7873.

(41) (a) Sabo-Etienne, S.; Rodriguez, V.; Donnadieu, B.; Chaudret, B.; Abou el Makarim, H.; Barthelat, J.-C.; Ulrich, S.; Limbach, H.-H.; Moise, C. *New. J. Chem.* **2001**, *25*, 55. (b) Sabo-Etienne, S.; Chaudret, B.; Abou el Makarim, H.; Barthelat, J.-C.; Daudey, J.-P.; Ulrich, S.; Limbach, H.-H.; Moise, C. *J. Am. Chem. Soc.* **1995**, *117*, 11602.

(42) (a) While no $^2J_{H-H}$ coupling is resolved between these hydrides in the room-temperature ^{1}H NMR spectrum, this is likely due to the quadrupolar broadening of these signals rather than the presence of any exchange coupling. Since the presence of the phenomenon has been linked with the availability of η^2-dihydrogen[39b] structures, its apparent absence in this system suggests that this intermediate is extremely short-lived. For systems where the exchange and magnetic coupling constants are similar in magnitude, Heinekey has shown that the *observed* coupling constant is extremely temperature sensitive. When samples of **1** are cooled to −60 °C, the signals for both the bridging and terminal hydrides sharpen somewhat (whh for the terminal hydride = 6 Hz at −60 °C), but coupling is still not apparent in this signal. Although the expected two-bond coupling constant of $\approx$10−13 Hz for a *cis* dihydride[ref] is therefore absent in this system, the most likely reason is the quadrupolar broadened nature of the signals involved, but we cannot rule out the presence of exchange coupling in this system with the available data. (b) Camanyes, S.; Maseras, F.; Moreno, M.; Lledos, A.; LLuch, J. M.; Bertran, J. *J. Am. Chem. Soc.* **1996**, *118*, 4617. (c) Gibson, V. C.; Bercaw, J. E.; Bruton, J. W., Jr.; Sanner, R. D. *Organometallics* **1986**, *5*, 976.

Scheme 5

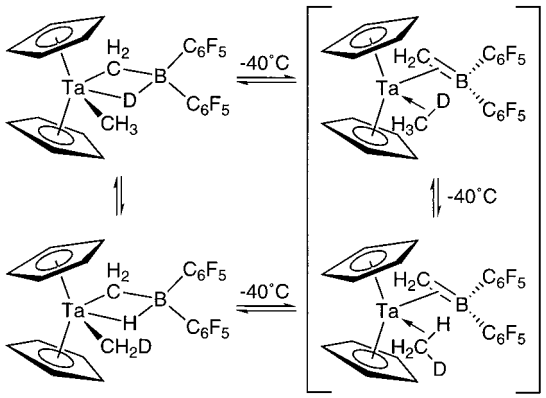

probably proceeds via a methane σ complex, as shown in Scheme 5. Methane σ complexes have been invoked in several studies to account for the transfer of label from the hydride position to the alkyl group in various alkyl hydrides $L_nM(D)CH_2R$, particularly in systems where the reductive elimination is endothermic.[18b,e,44] Slippage of the ground-state structure of **2** to an η^2/η^1-borataalkene species would allow the σ complex to form and mediate the scrambling prior to collapse back to the methyl hydride structure. We observe no deuterium incorporation into the methylene position of **2** because in the temperature regime where this would be expected to occur, methane elimination is facile.

Conclusions. Borataalkene complexes of tantalocene have been generated by reaction of $Cp_2Ta(=CH_2)CH_3$ with $HB(C_6F_5)_2$. The borataalkene ligand generated in this process, $[CH_2=B(C_6F_5)_2]^-$, flexibly binds the metal in either an η^1 alkyl-like mode or an η^2 alkene-like mode. This work raises the possibility of exploring the coordination chemistry of other borataalkene ligands and also whether these ligands show similar reactivity patterns to standard olefin ligands. In fact, in analogy to zirconium-mediated cyclization of olefins and alkynes,[45] we have observed that **3** may be trapped with alkynes to give tantallacyclopentene structures[46] and will report these results in due course.

Experimental Section

General Procedures. Unless otherwise noted all manipulations were carried out under argon using an Innovative Technology System One drybox and/or standard Schlenk techniques on double manifold vacuum lines.[47] Toluene, hexanes, and THF were dried and deoxygenated using the Grubbs/Dow solvent purification system[48] and were stored in evacuated glass vessels over titanocene[49] or sodium benzophenone. Deuterated NMR solvents d_6-benzene and d_8-THF were dried and distilled from sodium/benzophenone ketyl, and d_2-dichloromethane was dried and distilled from calcium hydride. NMR spectra were recorded on Bruker AC 200, AM 400, or AMX2 300 MHz spectrometers at room temperature and in C_6D_6 unless otherwise specified. Proton and carbon spectra were referenced to solvent signals, boron spectra to external $BF_3\cdot Et_2O$ at 0.0 ppm, and fluorine spectra to C_6F_6 at −163.0 ppm relative to $CFCl_3$ at 0.0 ppm. NMR data are given in ppm; ^{13}C resonances for the C_6F_5 groups were not obtained. Elemental analyses were performed in the microanalytical laboratory of the Department of Chemistry at the University of Calgary. $HB(C_6F_5)_2$,[11] $Cp_2Ta(=CH_2)(CH_3)$,[10] and $ClB(C_6F_5)_2$[50] were prepared by literature methods. *t*-BuNC was dried over molecular sieves prior to use. Carbon monoxide was passed through an Oxisord-W purification column before introduction to the reaction vessel.

Synthesis of $Cp_2Ta(CH_2B(C_6F_5)_2)(\mu\text{-}H)(H)$, 1. From $Cp_2Ta(=CH_2)(CH_3)$. Benzene (10 mL) was condensed into an evacuated flask containing $HB(C_6F_5)_2$ (286 mg, 0.828 mmol) and $Cp_2Ta(=CH_2)CH_3$ (141 mg, 0.414 mmol) at −78 °C. The solution was warmed to 25 °C and stirred for 1 h. Benzene was removed under reduced pressure and hexane (15 mL) condensed in at −78 °C. The light tan precipitate was isolated by filtration and washed by hexane (3 × 10 mL) through back distillation. Solvent was removed under reduced pressure. Yield of **1**: 221 mg, 0.329 mmol, 79%. X-ray quality crystals were grown from C_6H_6. **From 2, Method I.** Toluene (15 mL) was condensed into a 50 mL glass bomb containing methyl hydride **2** (370 mg, 0.539 mmol) at −78 °C. One atmosphere of H_2 was introduced to the cooled bomb and the bomb sealed. The solution was allowed to warm slowly overnight with vigorous stirring to give a light brown solution and transferred via cannula to a 50 mL round-bottom flask with filtering frit. Toluene was removed under reduced pressure to leave a tan residue. Hexanes (25 mL) was condensed in at −78 °C and the slurry sonicated to give a fine tan powder, which was filtered and washed with hexanes (3 × 10 mL) by back distillation. Hexanes were removed under reduced pressure. Yield of **1**: 270 mg, 0.401 mmol, 74%. **From 2, Method II.** Toluene (10 mL) was condensed into an evacuated flask containing methyl hydride **2** (296 mg, 0.431 mmol) and $HB(C_6F_5)_2$ (151 mg, 0.431 mmol) at −78 °C. The solution was slowly warmed to room temperature with stirring for 1 h to give a brown solution. Toluene was removed under reduced pressure and hexane (15 mL) condensed in at −78 °C. The tan precipitate was isolated by filtration and hexane removed under reduced pressure. Yield of **1**: 206 mg, 0.306 mmol, 71%. Anal. Calcd for $C_{23}H_{14}BF_{10}Ta$: C, 41.10; H, 2.10. Found: C, 40.87; H, 1.86. ^1H NMR: 4.35 (s, 10H, C_5H_5), 0.80 (s, 2H, CH_2), 0.15 (s, 1H, Ta-*H*), −3.27 (br s, 1H, Ta-*H*-B). ^{13}C NMR: 96.1 (C_5H_5), 6.9 (CH_2, $^1J_{CH}$ 147.2 Hz). ^{11}B NMR: −35.5. ^{19}F NMR: −129.4 (4F, *o*-F), −159.2 (2F, *p*-F), −163.7 (4F, *m*-F).

Synthesis of $Cp_2Ta(CH_2B(C_6F_5)_2)(\mu\text{-}H)(CH_3)$, 2. Hexanes (15 mL) were condensed into a flask containing $HB(C_6F_5)_2$ (307 mg, 0.882 mmol) and $Cp_2Ta(=CH_2)(CH_3)$ (302 mg, 0.882 mmol) at −78 °C. The solution was warmed to 25 °C and stirred for 45 min. The tan precipitate was isolated by filtration and washed with hexanes (3 × 5 mL) by back distillation. Solvent was removed under reduced pressure. Yield of **2**: 549 mg, 0.800 mmol, 90%. For d_1-**2** the borane $DB(C_6F_5)_2$ was utilized. For d_6-**2**, $DB(C_6F_5)_2$ and $Cp_2Ta(=CD_2)(CD_3)$ were employed. Suitable elemental analyses were not obtainable due to the instability of the compound at 25 °C. ^1H NMR (d_8-THF, −78 °C): 5.51 (s, 10 H, C_5H_5), 1.19 (s, 2H, CH_2), 0.82 (s, 3H, CH_3),

(43) An alternative formulation of **C** would be $Cp_2Ta[\eta^2\text{-}(H)(CH_3)B(C_6F_5)_2]$, i.e., an alkyl hydridoborate Ta(III) structure, which could collapse directly back to **1** via oxidative addition of one of the methyl group C−H bonds to the Ta(III) center.

(44) (a) Parkin, G.; Bercaw, J. E. *Organometallics* **1989**, *8*, 1172. (b) Gould, G. L.; Heinekey, D. M. *J. Am. Chem. Soc.* **1989**, *111*, 5502. (c) Wang, G. Ziller, J. W.; Flood, T. C. *J. Am. Chem. Soc.* **1995**, *117*, 1647. (d) Stahl, S. S.; Labinger, J. A.; Bercaw, J. E. *J. Am. Chem. Soc.* **1996**, *118*, 5961. (e) Wick, D. D.; Reynolds, K. A.; Jones, W. D. *J. Am. Chem. Soc.* **1999**, *121*, 3974. (f) Mobley, T. A.; Schade, C.; Bergman, R. G. *J. Am. Chem. Soc.* **1995**, *117*, 7822.

(45) Leading reference: Takahashi, T.; Huo, S.; Hara, R.; Noguchi, Y.; Nakajima, K.; Sun, W.-H. *J. Am. Chem. Soc.* **1999**, *121*, 1094.

(46) Cook, K. S.; Piers, W. E.; McDonald, R. Manuscript in preparation.

(47) Burger, B. J.; Bercaw, J. E. *Experimental Organometallic Chemistry*; Wayda, A. L., Darensbourg, M. Y., Eds.; ACS Symp. Ser. 357; American Chemical Society: Washington, DC, 1987.

(48) Pangborn, A. B.; Giardello, M. A.; Grubbs, R. H.; Rosen, R. K.; Timmers, F. J. *Organometallics* **1996**, *15*, 1518.

(49) Marvich, R. H.; Brintzinger, H. H. *J. Am. Chem. Soc.* **1971**, *93*, 2046.

(50) Chambers, R. D.; Chivers, T. *J. Chem. Soc.* **1965**, 3933.

Table 2. Summary of Data Collection and Refinement Details for 5

formula	$C_{24}H_{12}F_{10}BOTa$
fw	698.10
cryst syst	monoclinic
space group	$P2_1/c$
a, Å	8.1958(5)
b, Å	15.8023(9)
c, Å	16.6702(9)
β, °	94.1670(10)
V, Å^3	2153.3(2)
Z	4
d_{calc}, mg m^{-3}	2.153
μ, mm^{-1}	5.208
T, °C	-80
cryst dimens, mm^3	0.12 × 0.10 × 0.04
rel. transmn factors	0.8569−0.6507
2θ (max), deg	51.40
total data	11322
no. of ind reflns	4077
no. of observations[a]	3035
no. of variables	329
restraints	0
R_1, $F_o^2 > 2\sigma(F_o^2)$	0.0304
wR_2, $F_o^2 > 2\sigma(F_o^2)$	0.0518
R_1 all data	0.0505
wR_2 all data	0.0555
gof	0.900
residual density, e/Å^3	−0.871 to −0.846

[a] $F_o^2 \geq 2\sigma(F_o^2)$).

−1.54 (br s, 1H, B*H*). ^{13}C NMR (d_8-THF, −78 °C): 105.7 (C_5H_5), 20.5 (CH_2, $^1J_{CH}$), 1.2 (CH_3, $^1J_{CH}$). ^{11}B NMR (d_8-THF, −78 °C): −30.8 ppm. ^{19}F NMR (d_8-THF, −78 °C): −129.8 (2F, *o*-F), −132.7 (2F, *o*-F), −162.6 (2F, *p*-F), −165.6 (2F, *m*-F), −166.0 (2F, *m*-F).

$Cp_2Ta(\eta^2\text{-}CH_2B(C_6F_5)_2)(CNC(CH_3)_3)$, 4. Toluene (15 mL) was condensed into a flask containing **2** (524 mg, 0.778 mmol) at −78 °C. To this slurry, $(CH_3)_3CNC$ (0.26 mL, 2.30 mmol) was added dropwise at −78 °C. The solution was stirred for 1.5 h at room temperature, during which time a dark orange color developed. The toluene was removed under reduced pressure, and hexane (20 mL) was added to produce an orange slurry. The light orange precipitate was filtered and washed with cold hexanes (3 × 10 mL) by back distillation, and solvent was removed under reduced pressure. Yield of **4**: 491 mg, 0.652 mmol, 84%. X-ray quality crystals were grown from CH_2Cl_2. Anal. Calcd for $C_{28}H_{21}NBF_{10}Ta$: C, 44.65; H, 2.81; N, 1.79. Found: C, 44.69; H, 2.48; N, 2.26. IR: ν_{CN} 1882 cm^{-1}. ^{1}H NMR (CD_2Cl_2): 4.90 (s, 10H, C_5H_5), 1.41 (s, 9H, CH_3), 1.13 (s, 2H, CH_2). ^{13}C NMR (CD_2Cl_2): 94.3 (C_5H_5), 30.7 (CH_3), 9.1 (CH_2). ^{11}B NMR (CD_2Cl_2): 8.5. ^{19}F NMR (CD_2Cl_2): −127.4 (4F, *o*-F), −161.3 (2F, *p*-F), −166.4 (4F, *m*-F).

$Cp_2Ta(\eta^2\text{-}CH_2B(C_6F_5)_2)(CO)$, 5. Toluene (15 mL) was condensed into a 250 mL glass bomb containing intermediate **5** (350 mg, 0.510 mmol) at −78 °C. To the cold slurry 1 atm of CO was introduced and the vessel sealed. The solution was stirred vigorously for 1.5 h at room temperature, during which time the solution turned dark orange. The solution was transferred to a 50 mL round-bottom flask with filtering frit and toluene removed under reduced pressure to give an orange oil. Hexanes (20 mL) were condensed in at −78 °C, and the solution was sonicated to produce an orange precipitate. The light orange precipitate was filtered and washed with cold hexanes (3 × 10 mL) by back distillation. The solvent was then removed under reduced pressure. Yield of **5**: 292 mg, 0.427 mmol, 82%. X-ray quality crystals were grown from CH_2Cl_2. Anal. Calcd for $C_{24}H_{12}BOF_{10}Ta$: C, 41.29; H, 1.73. Found: C, 41.44; H, 1.86. IR: ν_{CO} 1923 cm^{-1}. ^{1}H NMR (CD_2Cl_2): 5.03 (s, 10H, C_5H_5), 1.06 (s, 2H, CH_2). ^{13}C NMR (d_8-THF): 254.5 (*C*O), 95.3 (C_5H_5), 9.3 (CH_2). ^{11}B NMR (CD_2Cl_2): 7.2. ^{19}F NMR (CD_2Cl_2): −128.3 (4F, *o*-F), −159.6 (2F, *p*-F), −165.0 (4F, *m*-F).

Kinetic Measurements of Methane Loss From 2. In a typical experiment, **2** (35 mg, 0.051 mmol) and ferrocene (internal standard, 5 mg, 0.027 mmol) were weighed into a sealable NMR tube. A known amount of THF-d_8 (0.731 g, 0.742 mL) was condensed in at −78 °C and the NMR tube flame sealed under vacuum at −78 °C. Kinetic data was obtained by following the disappearance of the cyclopentadienyl proton resonance in the ^{1}H NMR spectra generated with one pulse. Kinetic data for the observed kinetic isotope effect was generated using four pulses with a delay of 15 s between the pulses. Integration of the cyclopentadienyl resonance was determined versus the ferrocene standard normalized to 1.00 and the concentration of **2** calculated. First-order kinetic behavior is observed for greater than 3 half-lifes. All determinations were performed, minimally, in duplicate.

Computational Details. All Kohn−Sham density functional theory calculations were performed with the ADF2000.02 quantum chemistry package.[51] The gradient-corrected exchange functional of Becke[52] and the correlation functional of Perdew[53] were utilized in conjunction with the LDA parametrization of Vosko, Wilk, and Nusair[54] for the calculation of both the energy and gradients. An uncontracted triple-ζ basis of Slater-type orbitals was employed for the 5s, 5p, 5d, 6s, and 6p valence shells of the Ta center, which is designated as the IV basis in ADF. For the main group elements (including H), the ADF type III basis was used, which consists of double-ζ basis of Slater-type orbitals for the ns and np valence shells that are augmented with polarization functions. Inner shells were treated with the frozen core approximation. No symmetry constraints were used during geometry optimizations. Spin-restricted formalism was used for all calculations except for those on the intermediate complex **3**, where the unrestricted formalism was used. The expectation value of S^2 is not determined within the ADF package, and the amount of spin contamination was not measured for the unrestricted calculations. Quasi-first-order scalar relativistic corrections are utilized.[55] For the combined QM/MM calculations, the IMOMM approach as implemented within ADF was used.[56] For these calculations, the α ratio for the B−C link bonds were fixed to a value of 1.331. The Tripos 5.2 force field[57] was utilized for the molecular mechanics potential. Using the Tripos atomtype designations, torsional parameters for B−C_{ar} bonds were taken to be the same as the Tripos C_{ar}−C_{ar} torsional parameters. The van der Waals parameters for Ta and B from the UFF[58] force field were used.

X-ray Crystallography. Crystals of **5** were coated in Paratone-8277 oil; one of these was mounted on a glass fiber for diffraction measurements. Data were collected using a Bruker P4/RA diffractometer with a SMART 1000 CCD detector,[59] using monochromated Mo Kα radiation at −80 °C.

(51) (a) Scientific Computing & Modelling NV, V. U., Theoretical Chemistry, De Boelelaan 1083, 1081 HV Amsterdam, The Netherlands. (www.scm.com). (b) Baerends, E. J.; Ros, P. *Chem. Phys.* **1973**, *2*, 52. (c) Versluis, L.; Ziegler, T. *J. Chem. Phys.* **1988**, *88*, 322. (d) te Velde, G.; Baerends, E. J. *J. Comput. Phys.* **1992**, *99*, 84. (e) Fonseca-Guerra, C.; Snijders, J. G.; te Velde, G.; Baerends, E. J. *Theor. Chem. Acc.* **1998**, *99*, 391.

(52) Becke, A. *Phys. Rev. A* **1988**, *38*, 3098.

(53) (a) Perdew, J. P. *Phys. Rev. B* **1986**, *33*, 8822. (b) Perdew, J. P. *Phys. Rev. B* **1986**, *34*, 7406.

(54) Vosko, S. H.; Wilk, L.; Nusair, M. *Can. J. Phys.* **1980**, *58*, 1200.

(55) (a) Snijders, J. G.; Baerends, E. J.; Ros, P. *Mol. Phys.* **1979**, *38*, 1909. (b) Ziegler, T.; Tschinke, V.; Baerends, E. J.; Snijders, J. G.; Ravenek, W. *J. Phys. Chem.* **1989**, *93*, 3050. (c) van Lenthe, E.; Baerends, E. J.; Snijders, J. G. *J. Chem. Phys.* **1993**, *99*, 4597.

(56) (a) Woo, T. K.; Cavallo, L.; Ziegler, T. *Theor. Chem. Acta* **1998**, *100*, 307. (b) Maseras, F.; Morokuma, K. *J. Comput. Chem.* **1995**, *16*, 1170.

(57) Clark, M.; Cramer, R. D., III.; Van Opdenbosch, N. *J. Comput. Chem.* **1989**, *10*, 982.

(58) Rappé, A. K.; Casewit, C. J.; Colwell, K. S.; Goddard, W. A., III; Skiff, W. M. *J. Am. Chem. Soc.* **1992**, *114*, 10024.

(59) Programs for diffractometer operation, data collection, data reduction, and absorption correction were those supplied by Bruker.

(60) Sheldrick, G. M. *Acta Crystallogr.* **1990**, *A46*, 467 .

Data were integrated to a maximum 2θ value of 51.40° and were corrected for absorption through use of the SADABS procedure. The structure of **5** was solved using the program SHELXS-86,[60] and the structure was refined using full-matrix least-squares methods (SHELXL-93).[61] All non-hydrogen atoms were refined anisotropically, and all hydrogen atoms were placed in idealized positions as suggested by the sp^2 or sp^3 hybridizations of their attached carbons. Details of crystal data, data collection, and structure refinement have been provided in Table 2.

(61) Sheldrick, G. M. *SHELXL-93*. Program for crystal structure determination; University of Göttingen: Germany, 1993. Refinement on F_o^2 for all reflections (all of these having $F_o^2 \geq -3\sigma(F_o^2)$). Weighted R-factors wR_2 and all goodnesses of fit S are based on F_o^2; conventional R-factors R_1 are based on F_o, with F_o set to zero for negative F_o^2. The observed criterion of $F_o^2 > 2\sigma(F_o^2)$ is used only for calculating R_1 and is not relevant to the choice of reflections for refinement. R-factors based on F_o^2 are statistically about twice as large as those based on F_o, and R-factors based on all data will be even larger.

Acknowledgment. Funding for this work came from the Natural Sciences and Engineering Research Council of Canada in the form of Research Grants (to W.E.P. and T.K.W.), an E. W. R. Steacie Fellowship (2001−2003) (to W.E.P.), and Scholarship support (PGSA and PGSB) to K.S.C. K.S.C. also thanks the Steinhauer Foundation for a Fellowship (2000-2001). Prof. Tom Ziegler is also thanked for the use of the COBALT facility at the University of Calgary.

Supporting Information Available: Full listings of crystallographic data, atomic parameters, hydrogen parameters, atomic coordinates, and complete bond distances and angles for **5** plus Cartesian coordinates for calculated structures of **3** (singlet and triplet), **5** and **6**. This material is available free of charge via the Internet at http://pubs.acs.org.

OM010373O